



VERIFICATION OF SEISMIC STABILITY OF CAISSON TYPE BREAKWATER

Ryuzo OZAKI¹ and Takashi NAGAO²

SUMMARY

Seismic stability, which is on sliding and overturning, is verified for a design of a caisson type breakwater if necessary. In the present Japanese design code for the port and harbor, the evaluation of seismic stability of the breakwater is based on the static method called as the seismic coefficient method, which doesn't take the dynamic response of the breakwater into account.

In this study, the framework of the performance-based earthquake resistant design for caisson type breakwaters is presented. The procedure is as follows. The first step is to assess the necessity of the earthquake resistant performance by the schematic chart. The second step is to calculate the dimension of the breakwater for the evaluation of the earthquake resistant performance by the proposed method. The final step is to verify the earthquake resistant performance by the methodology based on a single degree of freedom system.

INTRODUCTION

When designing a breakwater, which is one of the major facilities of the port and harbor, the principal concern is its stability against waves, and its stability against earthquakes is often neglected (Technical Standards and Commentaries for Port and Harbour Facilities [1]). In contrast to quaywalls where loads directed toward the sea are dominant due to the action of earth pressure, with a breakwater there is no dominant loading action in a particular direction because the direction of loading action caused by inertial forces changes. The validity of the currently used design method has been proved by the fact that few breakwaters have suffered serious damage from strong motion during the past earthquakes. For example, the 1983 Nihonkai-chubu earthquake (Japan Society of Civil Engineers [2]) and the 1993 Kushiro-oki earthquake (Japan Society of Civil Engineers [3]) caused heavy damage to quaywalls and other port structures, but little to breakwaters. The 1994 Sanriku-haruka-oki earthquake (Research Committee on the Sanriku-haruka-oki Earthquake Damage [4]), however, caused the foundation to subside due to loss of rigidity. The 1995 Kobe earthquake caused subsidence of the ground and sliding of breakwaters on the

¹ Engineer, Chuo Fukken Consultants Co., Ltd., Osaka, Japan. Email: ozaki_r@cfk.co.jp

² Head of Port Design Standard Division, National Institute for Land and Infrastructure Management, Yokosuka, Japan. Email: nagao-t92y2@ysk.nilim.go.jp

order of 0.3m (Committee for Research Report on the Great Hanshin-Awaji earthquake [5] and Research Committee on the Great Hanshin Earthquake [6]).

Nevertheless, the earthquake resistant design of breakwaters is necessary, for example, in cases when design wave heights are low, and the caisson bodies do not need large weights for wave resistant stability. Since there has been no clear guideline on necessity of the earthquake resistant design of breakwaters, the decision has been left to the design engineers. Furthermore, the actual earthquake resistant design employs the seismic coefficient method that replaces the action of earthquake motion with static loading action. It also uses a safety factor to evaluate the safety. In view of the trend toward performance-based design method, however, the introduction of the reliability-based design (Ministry of Land, Infrastructure and Transport [7]) which can evaluate the safety of structure quantitatively, or the design method which can evaluate the response of the structure to loading action concretely is necessary. To streamline the earthquake resistant design, the next-generation Japanese design code for port and harbor focus on a design method to verify earthquake resistance based on the time history of earthquake ground motion (Nagao [8]). In this method, the design earthquake motion is not given by an area-wise seismic coefficient but by the time history of the engineering bedrock (the soil layer which has a shear wave velocity of 300-400m/s). We therefore need to construct an earthquake resistant performance verification system that can cope with future changes in how the design earthquake ground motion is expressed.

This paper describes a proposed framework for the earthquake resistant performance design of caisson type breakwaters. Our major objective is to provide a chart for assessing whether to verify earthquake resistant performance, a determination method of the cross sections for verification of earthquake resistant performance, and a method of checking earthquake resistant performance. For verifying earthquake resistant performance, we used a single degree of freedom system to evaluate the sliding and the overturning of breakwaters caused by earthquakes. Herein, we focus on the cases in which the rubble mound is not damaged during earthquakes.

FRAMEWORK OF THE EARTHQUAKE RESISTANT PERFORMANCE DESIGN OF BREAKWATERS

Verification Method

Figure 1 shows a flow for verifying the earthquake resistant performance of a breakwater. It is assumed that the earthquake resistant performance is verified after conducting the wave resistant design. We first assess whether the earthquake resistant performance needs to be verified based on the peak acceleration A_{max} of the engineering bedrock and the specification parameters of the caisson. If the result shows such verification is necessary, we compute the time history of the acceleration on the bottom surface of the breakwater caisson by the earthquake response analysis of ground. After calculating the seismic coefficient from the acceleration time history, we set the cross section for verifying the earthquake resistant performance by the seismic coefficient method. The next step is to compare the calculated caisson width B_{eq} of the cross section for verification with the width B_w obtained from the wave resistant design, and to choose the larger of the two as the caisson width for verification. Then a single degree of freedom system is used to calculate the earthquake response of the breakwater, such as the sliding and the overturning, and to verify the earthquake resistant performance. The step of setting the cross section for verification by means of the seismic coefficient method improves the efficiency of earthquake resistant performance verification. We need to develop the new items surrounded by thick-lined boxes in Figure 1. By the way, the performance required to the breakwater is to keep the port calm. Therefore, based on the past case examples, the limit state criterion of judgment with regard to the sliding is 50cm and the one to the overturning is 90degree in this study.

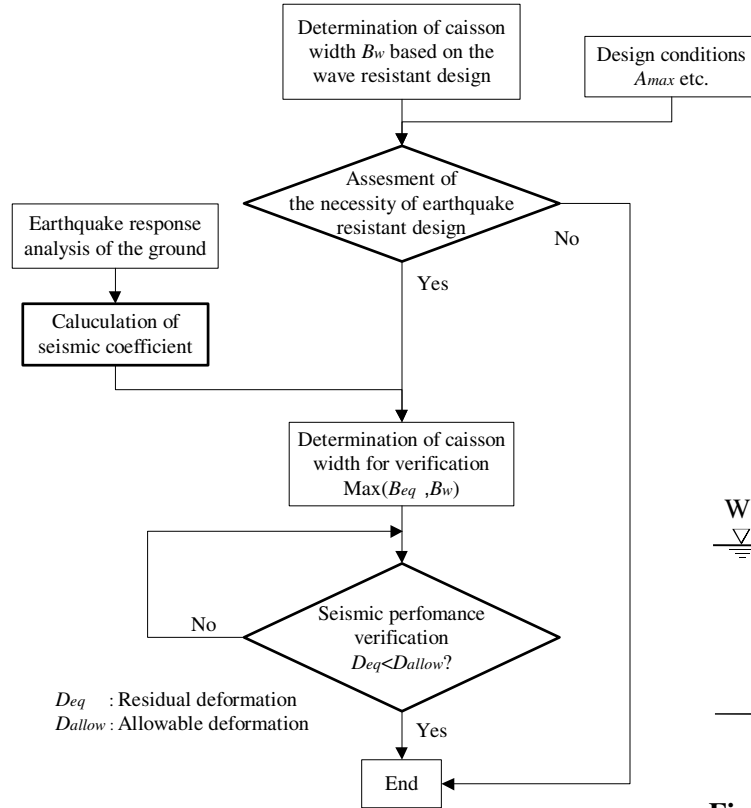


Figure 1 Flowchart for verifying the earthquake resistant performance of a breakwater

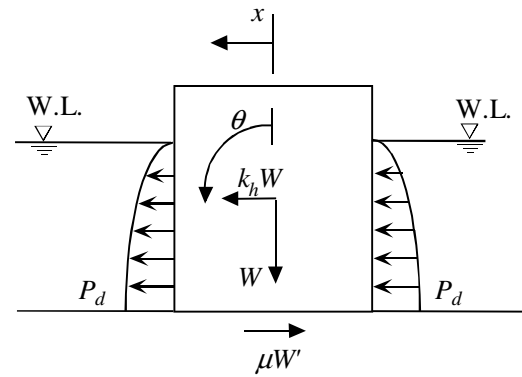


Figure 2 Load model of the breakwater

Method of Verifying Earthquake Resistant Performance

A single degree of freedom system of the breakwater caisson is applied to evaluate the earthquake response of the breakwater in order to verify the earthquake resistant performance. Sliding failure and overturning failure are considered as failure modes. We numerically integrated the equation of motion in a horizontal direction for the sliding mode, and the equation of angular motion around the edge of the bottom surface of the breakwater for the overturning mode (Sekiguchi [9]), when evaluating the earthquake response of the breakwater caisson based on Equations (1) and (2), respectively. Figure 2 shows the load model of the breakwater. The water level used in this study is the synodic averaged high water level (H.W.L.). This level gives the smallest ratio of the resistance force to the load effect. The friction coefficient μ between the concrete and the rubble is 0.6 (Technical Standards and Commentaries for Port and Harbour Facilities [1]).

$$\frac{W}{g} \frac{d^2 x}{dt^2} = k_h W + 2P_d - \mu W' \text{ (for the sliding safety)} \quad (1)$$

$$I \frac{d^2 \theta}{dt^2} = a k_h W + 2b P_d - c W' \text{ (for the overturning safety)} \quad (2)$$

$$\text{where, } P_d = \frac{7}{12} k_h \gamma_w H^2 \quad (3)$$

$$I = \frac{W}{g} \frac{(B^2 + h^2)}{3} \quad (4)$$

and

k_h : seismic coefficient ($=\alpha/g$)

α : acting acceleration (cm/s^2)

g : acceleration of gravity ($= 980\text{cm/s}^2$)

W : weight of the caisson of unit length (kN/m)

P_d : resultant dynamic water pressure of unit length (kN/m)

W' : effective weight of the caisson of unit length (kN/m)

H : water depth at the toe of caisson (m)

γ_w : unit weight of seawater (kN/m^3)

μ : friction coefficient between the caisson and the rubble mound

I : polar moment of inertia of unit length ($\text{kN} \cdot \text{m}^2/\text{m}$)

h : height of the caisson (m)

$a - c$: arm length of the load (m)

Application to One of the Disaster Cases Caused by the 1995 Kobe earthquake

We applied the method described in previous section to one of the breakwaters of Kobe port that was damaged during the 1995 Kobe earthquake, in order to examine the validity of the analytical method. The object of study is the seventh breakwater of Kobe port. It was located in an east-west direction roughly perpendicular to the dominant direction (north-south direction) of the earthquake. The survey conducted after the earthquake recorded a maximum displacement of 0.3m. No overturning occurred (Committee for Research Report on the Great Hanshin-Awaji earthquake [5]). Figure 3 shows the cross section of the breakwater.

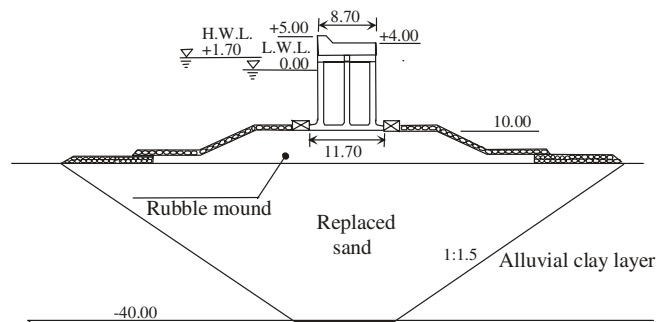


Figure 3 Cross section of the seventh breakwater of Kobe port

Based on the strong motion record at the point Kp-79m of Port Island obtained by Kobe City, we performed a one-dimensional equivalent linear earthquake response analysis, calculating the earthquake motion acting on the bottom surface of the caisson. After analyzing the NS (north-south) and EW (east-west) components, we obtained the component in a direction perpendicular to the breakwater, considering a direction error (Gifu Univ. [10]) that occurred at the time of placing the seismograph.

Figure 4 shows the time history of the earthquake motion on the bottom surface of the breakwater caisson and the caisson's response.

The long period wave was predominant due to the soft ground. As a result, the large displacement occurred at the peak acceleration

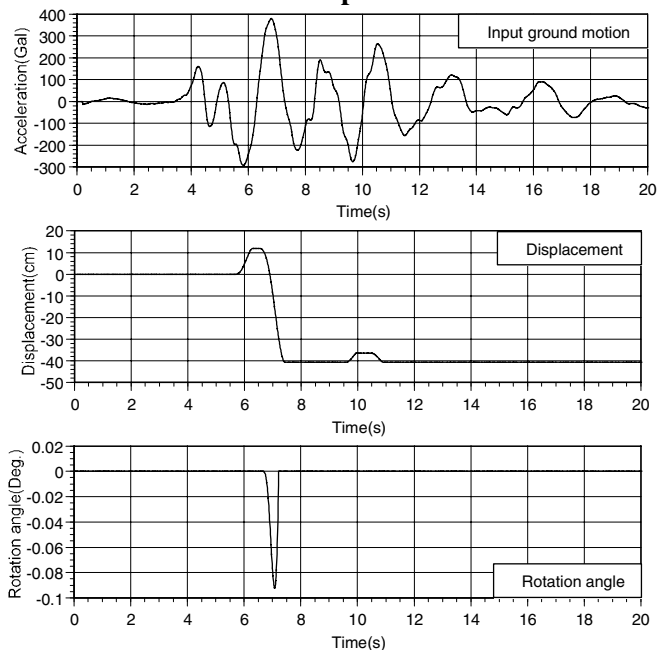


Figure 4 Input earthquake motion and caisson's response

amplitude of 7sec. The residual displacement was 0.4m, nearly matching the actual deformation. The rotation angle at the peak acceleration amplitude was only 0.1degree. The results thus proved the validity of our method.

METHOD OF ASSESSING THE NECESSITY OF EARTHQUAKE RESISTANT PERFORMANCE VERIFICATION

Study Method

As the constituent factors of the earthquake resistant performance verification system, we first studied the indices used for assessing the necessity of earthquake resistant performance verification. For the convenience of design engineers, we used the peak ground acceleration produced in the engineering bedrock instead of that on the bottom surface of the breakwater caisson. If it was judged to be unnecessary to verify the earthquake resistant performance, the response analysis of the ground could be omitted. Since the width of the caisson was decided in the wave resistant design, we studied an assessment method using the following two parameters as the indices: the ratio of the width to the water depth (B/H) and the peak ground acceleration on the engineering bedrock.

We selected the seven cross sections shown in Table 1 from the cross sections of breakwaters throughout Japan, maintaining a balance among the values of water depths and the conditions of the ground. Nine earthquake motions were used in total. The waves actually observed in port and harbor areas were the Hachinohe wave, the Ofunato wave, the Akita wave, and the Kobe wave used in previous chapter. The following simulated earthquake waves were also used: the strike wave and the dip wave caused by intraplate earthquakes; the subduction wave caused by interplate earthquake; and the earthquake motion representing the level-1 and the level-2 earthquakes used for the analysis of railroad structures (Railway Technical Research Institute [11]) (hereafter referred to as the JR1 wave and the JR2 wave, respectively).

The reasons why these nine waves were selected are followings. Based on the present standard, the waves that are applied to the earthquake resistant design are the Kobe, Hachinone, Ofunato and Akita waves, which have been recorded during the earthquakes in port and harbor. Since the synthesized waves taking the focal mechanism of earthquake, such as the intraplate and interplate earthquake, into account are adopted in next standard, the strike, dip and subduction waves are used. These waves were synthesized to consider the three types of the focal mechanism which are the intraplate lateral fault, reverse fault and interplate low angle reverse fault, respectively (Kagawa [12]). Furthermore, for the confirmation, the JR1 and JR2 waves are applied because these two are for the earthquake resistant design of railroad structures. Table 2 shows the dominant frequencies of these waves. Figure 5 shows the Fourier spectra of the acceleration of the Hachinohe, Kobe and the subduction wave as examples. The spectra were smoothed by a 0.3Hz bandwidth Parzen window and their peak amplitudes were adjusted to 100Gal· sec.

Table 2 Dominant frequencies of earthquake waves used for the study

	Predominant frequency(Hz)
Hachinohe wave	0.39
Ofunato wave	2.34
Kobe wave	2.88
Akita wave	0.44
Strike wave	1.66
Dip wave	0.68
Subduction wave	0.60
JR1 wave	0.78
JR2 wave	1.34

Table 1 Cross sections used for the study

	Water depth (-m)	Caisson width(m)	Front width of mound(m)
case1	11.5	7.5	6.5
case2	8.9	6.6	6
case3	12.2	5.5	6.5
case4	11.1	9.5	11
case5	11.8	7.5	5
case6	9.05	5	3.5
case7	11.05	5	4.5

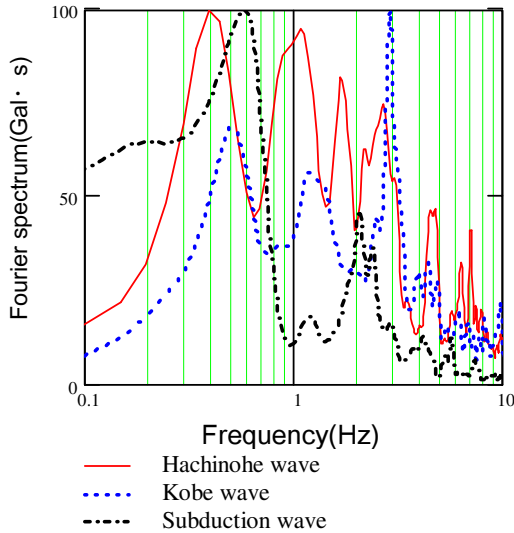


Figure 5 Fourier spectra of the acceleration

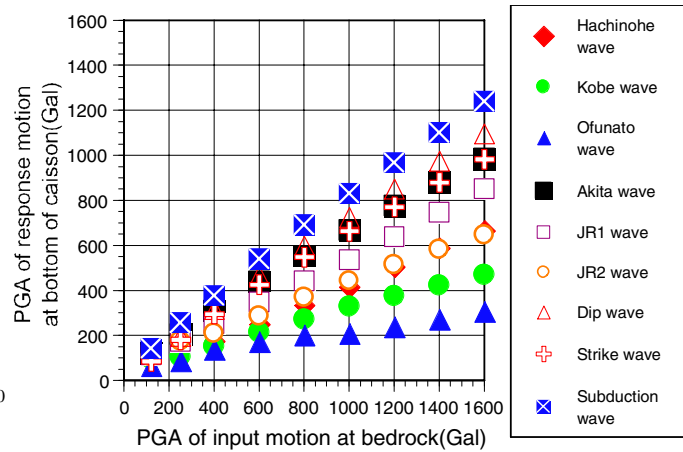


Figure 6 Relationship between PGA on bedrock and PGA of response motion of bottom surface of the caisson

As for the analysis, the peak acceleration amplitudes were adjusted to 120, 250, 400, 600, 800, 1000, 1200, 1400, and 1600 Gal of 2E wave (which has twice amplitude of incident wave), and the one-dimensional equivalent linear earthquake response analysis code Dyneq (Yoshida [13]) was used to calculate the earthquake motion produced on the bottom surfaces of the breakwater caissons for each cross section shown in Table 1. Figure 6 shows the relationship between the PGA on the bedrock, and that of the bottom surface of the breakwater caisson, using case 1 as an example. The amplification factors of the PGA were small due to the soft ground. The differences in the amplification factors of different waves were large. The acceleration amplification factor of the subduction wave was the highest, and that of the Ofunato wave was the lowest. The other cases showed similar results.

We next changed the caisson width by a step of 0.5m from the original design caisson width, using the single degree of freedom system shown in previous chapter to evaluate the response of the breakwater caisson. Figure 7 shows the contour maps of the residual displacements caused by the subduction wave (a), the Hachinohe wave (b), and the Kobe wave (c), focusing on case 6. The horizontal axis represents the ratio of the caisson width to the water depth (B/H), and the vertical axis the peak acceleration on the engineering bedrock. Figure 7 indicates that different waves give different displacement deformations even under the same condition of the peak bedrock acceleration and that the subduction wave gave the largest residual displacement. One of the reasons is that the acceleration amplification factor of the subduction wave was the highest, as shown in Figure 6. Another reason is that the direction of the sliding deformation of the breakwater caisson caused by the subduction wave did not change often in response to the change of the direction of the inertial force. Next chapter describes the difference in the patterns of sliding of the breakwater.

Even when the residual displacement of the caisson was very small, there was a possibility that a very large displacement was produced during the earthquake, causing the breakwater caisson to slip down the rubble mound. We hence studied the relationship between the residual displacement of the caisson and the maximum displacement in the earthquake-responding process. The results showed that the percentage of the maximum displacement caused by the Kobe wave was the largest with respect to the residual displacement. Figure 8 shows the contour map of the maximum displacements caused by the Kobe wave of case 6. The residual displacement necessary for breakwater caissons to be classified as disaster-stricken is usually about 50cm, but comparison with Figure 7 (c) indicates that in some cases, maximum

displacements of about 150cm were produced when the residual displacements were smaller than about 50cm. In other cases, maximum displacement of 400cm were sometimes produced when the residual displacements were 50cm, but all of them remained within the front width of the mounds shown in Table 1 and were not large enough to cause the caisson to slip down the mounds. It is therefore concluded that we only need to consider the residual displacement when evaluating the sliding failure for judging the necessity of earthquake resistant performance verification. The maximum deformations of about 400cm were produced when the PGA were about 1000Gal. With different earthquake waves, the PGA smaller than 1000Gal gave a residual displacement exceeding 50cm.

We then compared the sliding failure with the overturning failure, and found that the overturning failure only occurred when the PGA was very large. As results of studies by the ground motion giving stricter conditions of overturning than those of sliding, focusing on the subduction wave (see Figure 9) showed that overturning only occurred when the ratios of the caisson width to the water depth (B/H) were extremely small and the produced residual displacements were larger than about 300cm. We therefore concluded that the conditions for overturning breakwaters did not need to be verified, and so the following sections focus on sliding failure.

Figure 10 shows the conditions for each of the studied breakwater cross sections, with the change of the caisson width by a step of 0.5m from the original design caisson width, to cause the subduction wave to produce a residual displacement of larger than 50cm. The values of case 6 represent the lower limits. The curve connecting the lower limits is the assessment criterion of verifying the sliding failure of the breakwater. Even when the ratio of the caisson width to the water depth (B/H) reached 2.0, sliding failures were produced under certain conditions. This was because the increase of the caisson width caused the increase of the sliding resistance force as well as the increase of the inertial force. For reference, Figure 10 also shows the lower limit values for the Hachinohe wave to produce a residual displacement of 50cm. Since the lower limit curves depend largely on the earthquake motions, attentions should be paid when using other waves.

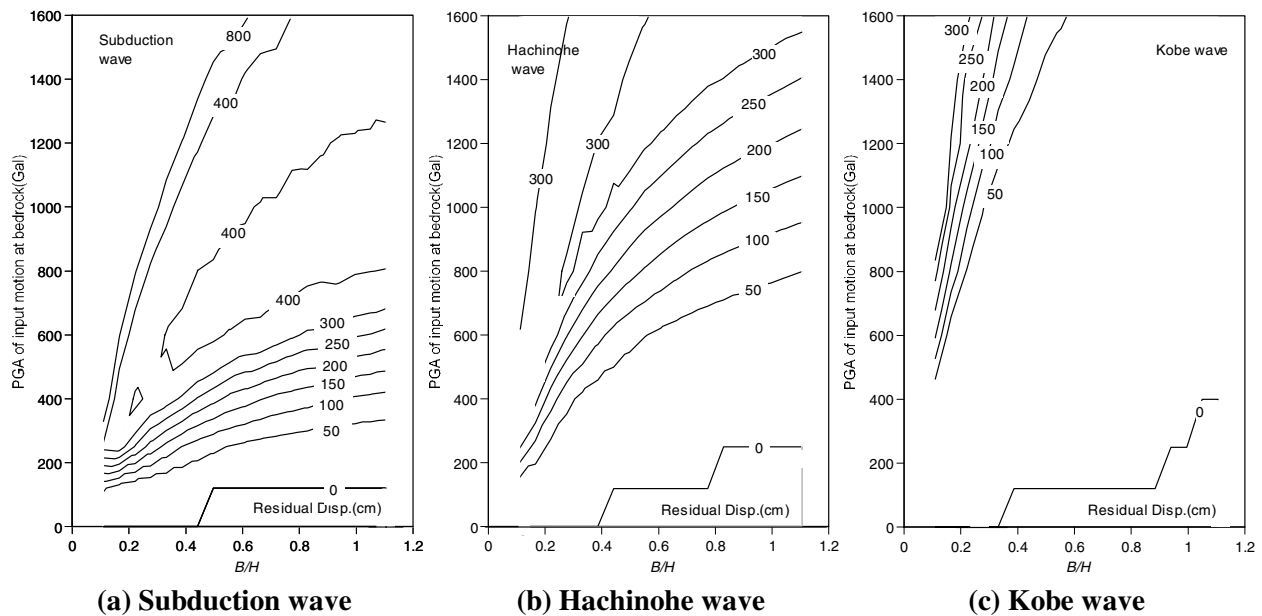


Figure 7 Relationship between peak bedrock acceleration and sliding failures

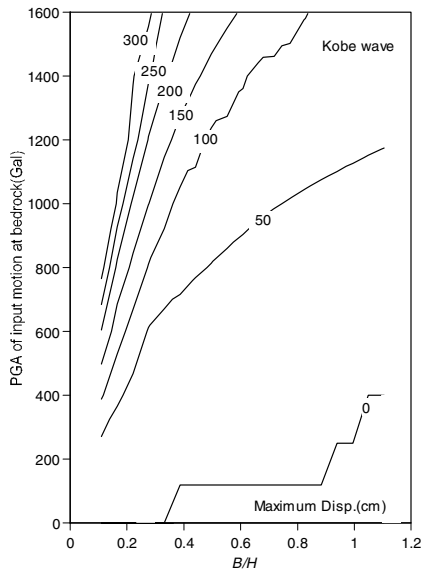


Figure 8 Relationship between peak bedrock acceleration and sliding failures (Maximum displacement of Kobe case)

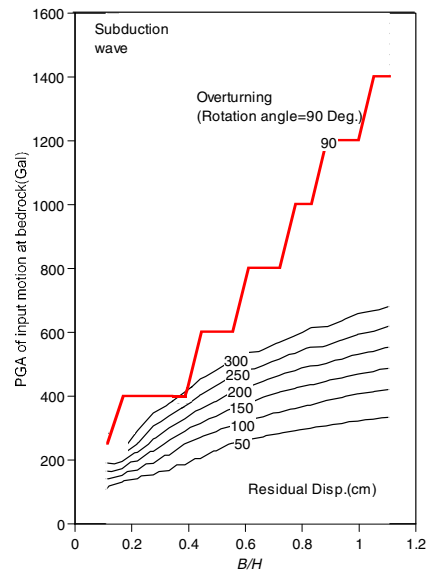


Figure 9 comparison between the sliding failure and the overturning failure

PROCEDURE FOR SETTING THE CROSS SECTIONS FOR VERIFICATION

Comparison between Residual Displacement and Maximum Displacement

The next subject is setting the cross section for verification when it is judged that the earthquake resistant performance of a breakwater needs to be verified. The basic procedure is to use the caisson width calculated from the result of the wave resistant design to verify the earthquake resistant performance. If the resultant displacement exceeds the assessment criterion, the next step is to increase the caisson width and repeat the calculation. This procedure is repeated until the optimum solution is obtained. For design engineers' convenience, we studied another method of setting the optimum cross section for verification.

As already examined in Figure 7, the relationship between the PGA on engineering bedrock and the residual displacement of the caisson differed largely depending on the input motions, so we studied the relationship between the PGA of the bottom surface of the caisson and the residual displacement. Using the Hachinohe wave, the Kobe wave, the JR2 wave, and the subduction wave under the conditions of case 1 ($B/H = 0.65$), we plotted in Figure 11 the relationship between the ratio of the caisson width to the water depth (B/H) and the PGA on the bottom surface of the caisson when the residual displacement of the breakwater caisson was 50 cm. This figure shows that the relationship between the PGA on the bottom surface of the caisson and the residual displacement also differed greatly depending on the ground motions. The other cases gave similar results. We conclude that it is inappropriate to use the PGA on the

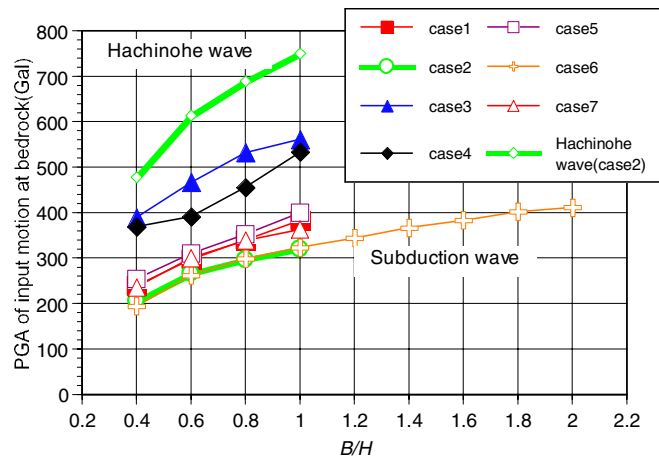


Figure 10 Chart for assessing the necessity of verifying earthquake resistant performance

bottom surface of a breakwater caisson for calculating the seismic coefficient directly. We tried to study the application of the peak velocity amplitudes and obtained the same result.

Focusing on cases 1 and 4 which have the contrasting ground condition with each other, we analyzed the reason in detail, using Figure 12. We plotted the time histories of the earthquake motion on the bottom surfaces of the caissons and those of the displacements of the breakwaters, with the PGA of input motion adjusted to give a residual displacement of 40cm. Figure 13 shows the Fourier amplitude spectra of the input motion on the bottom surfaces of the caissons. From the frequency characteristics shown in Figure 13, we found that the Fourier amplitude spectrum of the Kobe wave was dominant at all frequencies except the low frequency side of case 4. Since the residual displacements were the same, the frequency characteristics alone cannot evaluate the amount of residual displacements.

In the case of the residual displacement caused by the Hachinohe wave of case 1 shown in Figure 12, the first and the second displacement accumulated to form the residual displacement. In the case of the subduction wave, the shape of the residual one was formed almost at once. In the case of the Kobe wave, repeated positive and negative deformation formed the residual displacement, which was smaller than the maximum one. The waves showed no specific tendencies. For example, in the case of the Hachinohe wave of case 4, the residual displacement was formed almost at once.

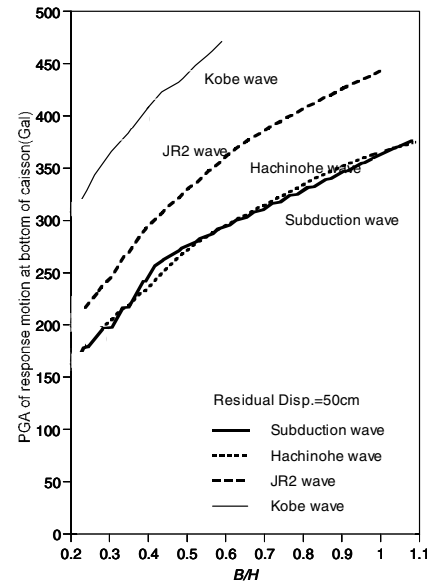


Figure 11 Relationship between the PGA on the bottom surface of the caisson and the residual displacement

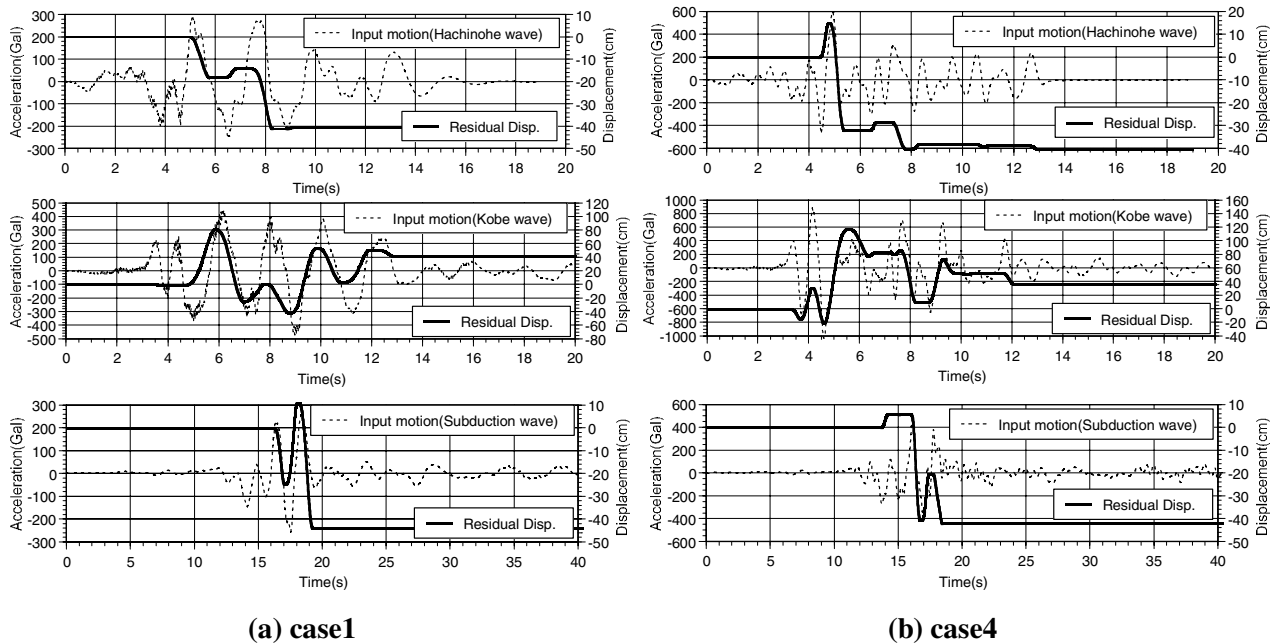


Figure 12 Input motion on the bottom surface of the breakwater and the deformation of the breakwater

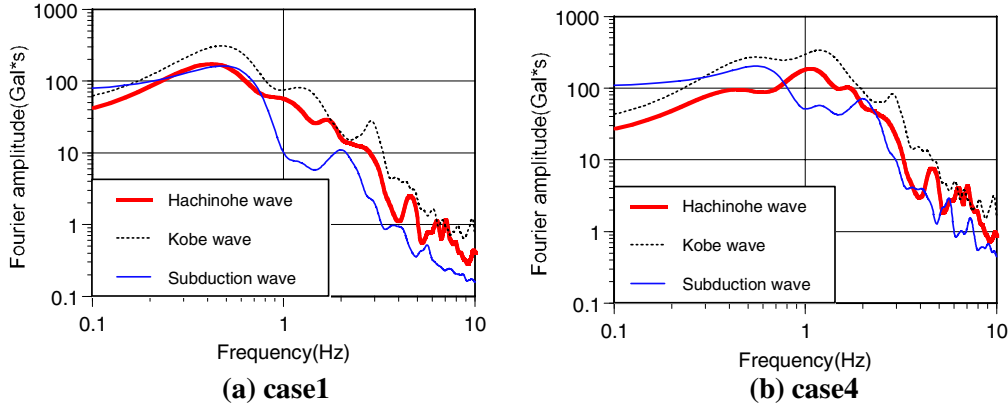


Figure 13 Fourier spectrum of the input motion on the bottom surface of the breakwater

Clearly, the preliminary estimation of the relationship between the maximum displacement and the residual one is important for properly verifying earthquake resistant performance. This study of all cases showed that the ratio of the residual displacement and the maximum displacement (R_{def}) can be estimated from the result (R_{acc}) of dividing the absolute value of the sum of the positive and negative peak acceleration amplitudes (acc_{max} and acc_{min} , respectively) by the larger one of the absolute values of those. As shown in Figure 14, we defined the maximum value of the differences between the variable points of the displacement vectors as the maximum displacement. R_{acc} is expressed as:

$$R_{acc} = \frac{|acc_{max} + acc_{min}|}{\max(|acc_{max}|, |acc_{min}|)} \quad (5)$$

Figure 15 shows the relationship between R_{acc} and R_{def} . Considering that the limit state criterion of judgment with regard to the sliding is 50cm, the 106 cases in which the residual displacement lie between 30 and 100cm were picked up from our studied all cases. Although the data were widely scattered, R_{def} tended to increase as R_{acc} increased. Using the result of linear regression of the relationship between the two (the straight line in the figure and Equation (6)), we estimate R_{def} from the acceleration time history.

$$R_{def} = 0.87R_{acc} + 0.44 \quad (6)$$

We also conducted a multiple regression including not only R_{acc} but also indices such as the dominant frequency, but the correlation coefficient did not increase significantly, so we estimated R_{def} from the positive and negative peak acceleration alone for simplification and convenience.

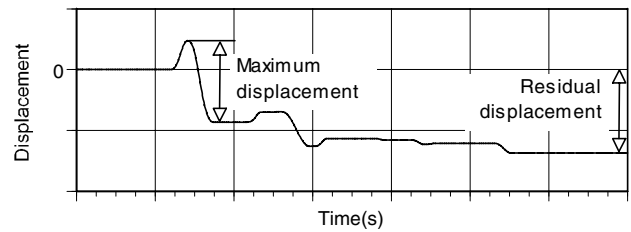


Figure 14 Definition of the maximum deformation

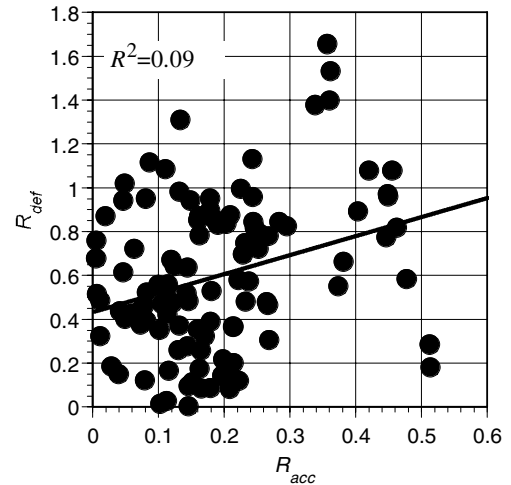


Figure 15 Relationship between R_{acc} and R_{def}

Procedure for Setting the Cross Sections for Verification

We then studied the procedure for setting the cross section of breakwater caissons for verification. Since we could estimate the target maximum displacement for the target residual displacement (50cm) from the acceleration time history of the bottom surface of a breakwater caisson, we studied the method of estimating the cross section necessary for producing the target maximum displacement. Instead of using actual earthquake waves having various frequency components, we used sine waves for our study.

As shown in Figure 16, we examined the peak acceleration amplitude necessary for giving a predetermined value of D_{max} . One cycle's displacement due to the sine wave would be almost constant after the third to fifth cycle. However, the maximum displacement of an actual breakwater caisson caused by an earthquake could not occur in the constant condition. Therefore, the displacement due to the second cycle was regarded as the maximum displacement D_{max} here. The study conditions were set as follows: frequency of earthquake motion = 0.1–10Hz; and B/H for cross section of breakwater caisson = 0.4, 0.6, and 0.8 (in case 1). We first examined the peak acceleration amplitudes that produced a value of D_{max} of 25-200cm. Figure 17 shows the results for D_{max} of 25cm. Different values of B/H of the breakwater gave different peak amplitudes. Dividing the amplitudes by the acceleration of gravity, and dividing the resultant by a limit seismic coefficient corresponding to a safety factor of displacement of just over 1.0, we obtained the values (R_{kh}) shown in Figure 18. The relationships were almost constant regardless of the values of B/H . The relationships are expressed as:

$$R_{kh} = a(D_{max})f^2 + b(D_{max})f + 1$$

$$a(D_{max}) = 0.0178D_{max} - 0.0035$$

$$b(D_{max}) = 0.0095D_{max} + 0.8174$$
(7)

where, f = frequency (Hz).

Since this study used a sinusoidal earthquake wave, the values of R_{kh} in Figure 18 correspond to the Fourier spectra of the acceleration. We multiplied the Fourier spectrum of the acceleration on the bottom surface of the breakwater caisson by a filter F so as to make the amplitude at each frequency the same as that at a frequency of 0Hz (1.0). We then obtained the spectrum (uniform-target maximum displacement spectrum)

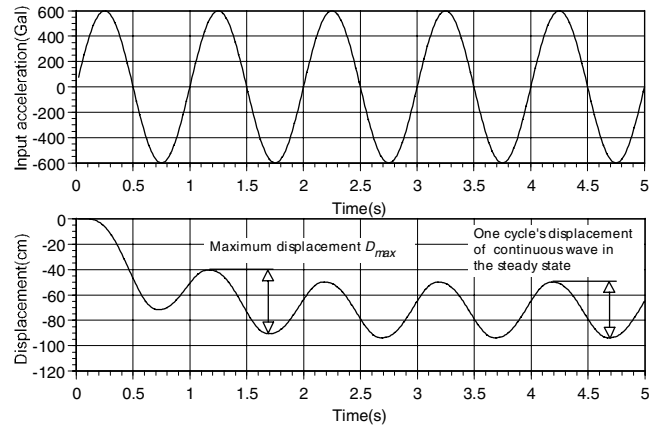


Figure 16 Study method

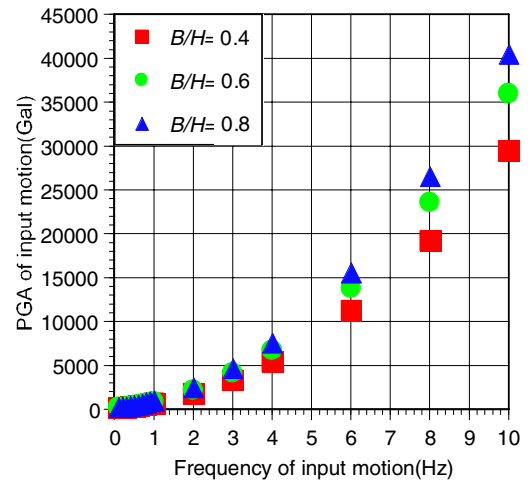


Figure 17 PGA of input motion against frequency

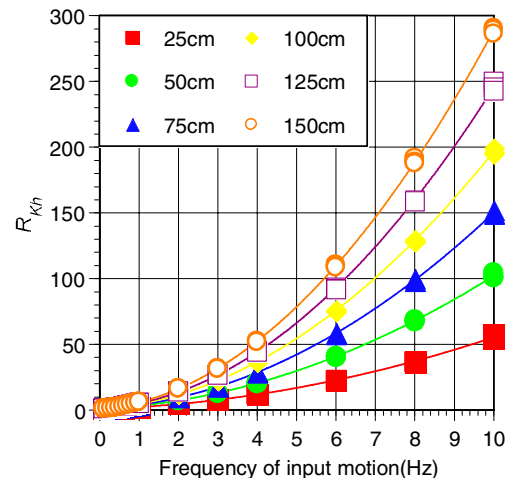


Figure 18 Seismic coefficient ratio against frequency

corresponding to the target maximum displacement at any frequency component. From the reciprocal plot of Equation (7), the filter F is expressed as (See Figure 19):

$$F = \frac{1}{a(D_{\max_t})f^2 + b(D_{\max_t})f + 1} \quad (8)$$

where,

D_{\max_t} : target maximum displacement (cm)

f : frequency (Hz)

$a()$, $b()$: same with Equation (7).

Multiplying the spectrum of an actual earthquake motion by this filter and performing inverse-Fourier transformation, and dividing the resultant peak acceleration amplitude by the acceleration of gravity, we can obtain the seismic coefficient for verification corresponding to the target displacement. Figure 20 shows the flow of calculating the seismic coefficient for verification.

Verification of the Validity of the Proposed Method

Here we verify the validity of the method of setting the cross section for verification described above. Using our method to calculate the seismic coefficient for verification on the 106 cross sections in which the correlation between R_{acc} and R_{def} was examined shown in Figure 15, we set the cross section giving a safety factor of 1.0 by using the calculated seismic coefficient. We then evaluated the displacement of the breakwater caisson having the cross section set above.

Figure 21 shows the relationship between the peak acceleration on the bottom surface of the breakwater caisson and the caisson weight ratio (R_{weight}) of the cross section for the verification of the earthquake resistant performance to that for the wave resistant design. Different symbols were used depending on whether the residual displacements were less than 50cm. In the cases where $R_{weight} < 1.0$, the verification was actually made based on the cross section obtained from the wave resistant design, i.e. based on the cross section in the case of $R_{weight} = 1.0$. It is clear from the figure that some of the values of R_{weight} calculated by the proposed method were equal to or larger than 3.0. Further study showed that the displacements produced in such cases were smaller than the target amount of 50cm, giving uneconomical cross sections. It is therefore appropriate to set the upper limit of R_{weight} at about 3.0 after calculating the caisson width from the seismic coefficient for verification.

We thus calculated the residual displacements for the modified caisson weights in the range of $1.0 \leq R_{weight} \leq 3.0$. Figure 22 shows the frequency distribution of the residual displacements. The residual displacements were distributed in a relatively narrow range of 0-100cm. The resultant average residual deformation was about 40cm, which was slightly smaller than the target amount of 50cm. This was influenced by the cases where the cross sections designed from the standpoint of wave resistance were larger than those designed from that of earthquake resistance. Also, there are some cases in which the

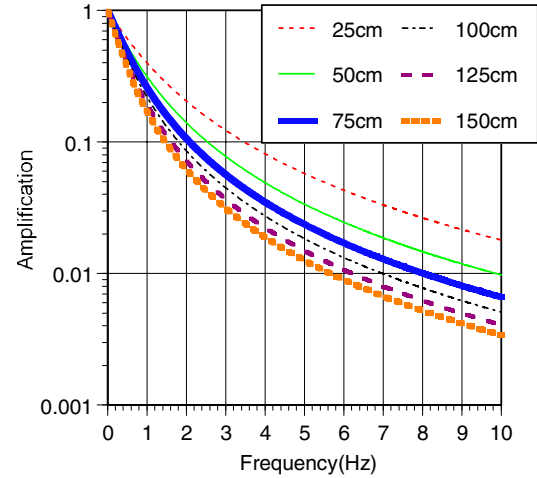


Figure 19 Filter for calculating the seismic coefficient for verification

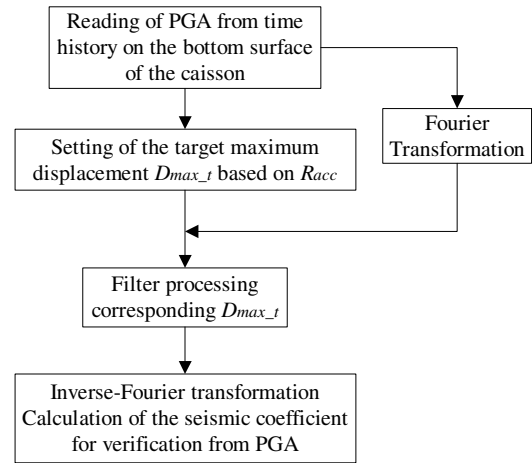


Figure 20 Flowchart for calculating the seismic coefficient for verification

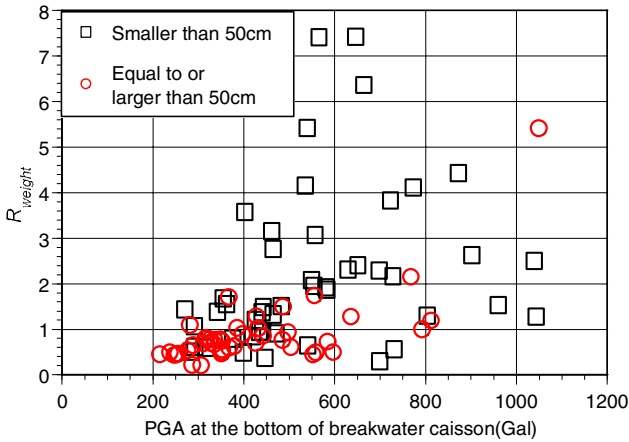


Figure 21 Relationship between the peak acceleration produced on the bottom of the breakwater and R_{weight}

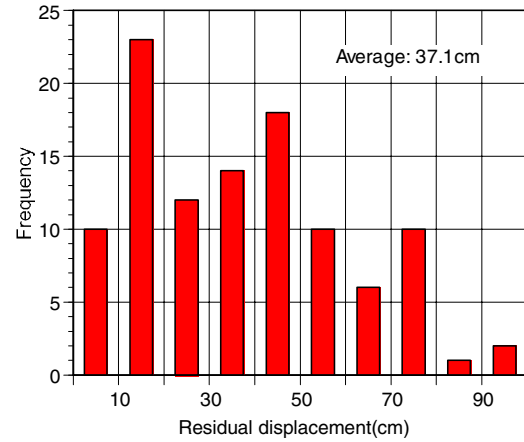


Figure 22 Frequency distribution of the residual displacement

residual displacement is much larger than 50cm. In such cases, it is necessary to repeat the procedure until the optimum solution is obtained.

As shown in Figure 15, the procedure of setting the cross sections for verification has 50% of possibility that the residual displacement would be over the allowable displacement of 50cm. In other words, it is difficult to determine the optimum cross section without some trial and error, because the data were widely scattered in Figure 15. However, it is possible to estimate the cross section required from the aspects of seismic stability with some degree of accuracy and to verify the earthquake resistant performance conveniently. In contrast with our proposed method, the numerical analysis approach by Equation (1) needs to repeat lots of trial and error in order to obtain the optimum cross section.

CONCLUSIONS

This paper shows the methodology of performance-based design for seismic stability of the caisson type breakwater. The conclusions are summarized as follows.

- 1 A method of verifying the earthquake resistant performance of caisson type breakwaters is developed. The method uses a single degree of freedom system to evaluate the sliding and overturning deformation of caissons. Using the method, we successfully evaluated the response of one of the breakwaters of Kobe port during the 1995 Kobe earthquake.
- 2 A chart for assessing whether the earthquake resistant performance of a breakwater needs to be verified is prepared. The assessment chart uses the PGA on the engineering bedrock and the ratio of the caisson width to the water depth. The failure mode of the breakwater is assumed to be sliding, as the overturning mode is not regarded to be a dominant factor.
- 3 The method of setting the cross section for verification is described when earthquake resistant performance needs to be verified. Using the positive and negative peak values of the acceleration on the bottom surface of the breakwater caisson to set the target maximum displacement, we calculated the seismic coefficient corresponding to the target maximum displacement.
- 4 Using the results above, we proved the effectiveness of the verification of the earthquake resistant performance of caisson breakwaters. The upper limit of the caisson weight ratio of the cross section

for the verification of the earthquake resistant performance to that obtained from the wave resistant design is 3.0.

The results of this study will be useful for the rational earthquake resistant design of breakwaters, which has traditionally been based on the method that the earthquake response of the breakwaters are not taken into account. When this report was written, area-wise earthquake motion was not given in the form of a time history. Design engineers who use this method should therefore select an earthquake motion for performance verification after examining differences in the earthquake responses of the caisson produced by different motions.

ACKNOWLEDGMENT

We are grateful to Mr. Masaki Fujimura, a researcher at the National Institute for Land and Infrastructure Management, for his help with the analysis.

REFERENCES

1. The Overseas Coastal Area Development Institute of Japan, "Technical Standards and Commentaries for Port and Harbour Facilities in Japan," 1999
2. Japan Society of Civil Engineers, "Research Report on the 1983 Nihonkai-chubu Earthquake Damage," 1986
3. Japan Society of Civil Engineers, "Research Report on the 1993 Kushiro-oki Earthquake Damage," 1994
4. Research Committee on the Sanriku-haruka-oki Earthquake Damage, "Research Report on the 1994 Sanriku-haruka-oki Earthquake Damage," The Japanese Geotechnical Society, 1996
5. Committee for Research Report on the Great Hanshin-Awaji earthquake, "Research Report on the Great Hanshin-Awaji earthquake: Damage to Civil Engineering Structures," Chapter 5: Port, Harbor, and Coast Structures, Japan Society of Civil Engineers, 1997
6. Research Committee on the Great Hanshin Earthquake, "Research Report on the Great Hanshin Awaji Earthquake: Reference Materials," Vol. 1, The Japanese Geotechnical Society, 1996
7. Ministry of Land, Infrastructure and Transport, "Basis of the Design on Civil Engineering and Architecture", 2002
8. Nagao T. "Trend in the Revision of the Standards for Port and Harbor Facilities," Proceedings of the 5th Symposium on Steel Structures and Bridges, Steel Structure Committee, The Japan Society of Civil Engineers, 2002: 9-20
9. Shibata T. and Sekiguchi H. "Bearing Capacity of the Ground," Kajima Institute Publishing Co., Ltd., 1995
10. Civil Engineering Department, Gifu University and Development Bureau, Kobe City, "Analysis of the Strong Motion Record at the Vertical Array Observation Point of Port Island," 1995
11. Railway Technical Research Institute, "Design Standards for Railway Structures: Earthquake Resistant Design," Maruzen Co., Ltd., 1999
12. Kagawa T. and Ejiri J. "Estimation of Ground Motion in Near-Field of Focal Region considering the Rupture Process of Causative Fault" Proceedings of Symposium Discussing the Level-2 Ground Motion for the Seismic Design of Soil Structure, 1998: 1-6
13. Yoshida N. and Suetomi I. "DYNEQ: Earthquake Response Analysis Program Based on the Equivalent Linear Method for the Horizontal Stratification Ground," Technical Laboratory Report, Sato Kogyo Co., Ltd., 1996: 61-70